A simple method for contact modelling in an arbitrary frame of reference within multi-physics software

Espino, Daniel; Shepherd, Duncan; Hukins, David

DOI:
10.1017/jmech.2012.128

—Technical Note—

A SIMPLE METHOD FOR CONTACT MODELLING IN AN ARBITRARY FRAME OF REFERENCE WITHIN MULTI-PHYSICS SOFTWARE

D. M. Espino * **D.E.T. Shepherd** **D.W.L. Hukins**

School of Mechanical Engineering
University of Birmingham
Birmingham, UK B15 2TT

ABSTRACT

A method to simulate contact between two boundaries of structures which are not aligned to predefined axes when using Comsol Multi-physics (v3.3, Comsol Ltd, Cambridge, UK) is presented. This method was developed because of limitations in the existing default contact modelling. Some of these limitations were recently addressed in a separate study; however, the method exploited symmetry across an axis of the coordinate system. The method presented here enables contact modelling with arbitrarily aligned structures within such a coordinate system. The contact method presented is then applied to a simple model with two deformable structures that come into contact, and compared over a range of positions. Results show a minimal variation in peak stress and contact pressure with model orientation, demonstrating that results are independent of orientation. Therefore, the contact method enables contact simulations in Comsol Multi-physics without assuming symmetry about an axis for contract. The method is compatible with the true transient contact method defined.

Keywords: Contact modelling, Finite element analysis, Hertzian contact, Large strain.

1. INTRODUCTION

This paper presents a method to define contact of boundaries from two structures which are not aligned to the predefined axes, in Comsol Multi-physics (v3.3, Comsol Ltd, Cambridge, UK). This finite element analysis (FEA) package, currently, enables contact modelling but it suffers certain limitations. For example, it assumes that time-dependency is equivalent to a range of steady state solutions where time is considered as a constant for each independent solution (*e.g.* to determine loading conditions). To solve this limitation, we previously reported a method to enable true time-dependent contact analysis for structures undergoing large strain [1]. This method was developed because Comsol multi-physics enables simultaneous multi-physics solutions. For example, we then applied the transient contact method to both a generalised Fluid-Structure Interaction (FSI) model [2] and to an FSI model of the mitral valve within the left ventricle of the heart [3]. However, in its current form the developed contact method exploits symmetry about an axis of a predefined Cartesian coordinate system. A method that enables contact in a model arbitrarily aligned within a coordinate system has not yet been described for this contact method.

The aim of this paper is to provide a contact method between boundaries without the need to exploit symmetry across a predefined axis. The implementation is defined for Comsol Multi-physics. The contact method is applied to a simple two-dimensional model resembling our previous heart valve contact model [1]. The model is solved for arbitrary positions in the coordinate system.

2. METHODS

2.1 Overview

The existing contact method and the modified contact method for arbitrary positioning within a Cartesian coordinate system are presented in section 2.2. The adapted contact method presented is then applied to a simple model used previously to define contacting components of a natural heart valve [1]. Sections 2.3 ~ 2.7 provide brief details of the model solved, but further explanation of the analysis is provided elsewhere [1]. For the analysis, the model (Fig. 1) was rotated (about the *x*-axis) at a range of angles to test the contact method works regardless of alignment to a predefined axis. Figure 2 shows both the un-rotated model and the model when rotated by 255°. Note, the contact method described assumes negligible surface sliding between contacting boundaries [2]; however, the equations used are also suitable for contact modelling where this is not the case [1].

* Corresponding author (daniel.m.espino@gmail.com)

DOI : 10.1017/jmech.2012.128

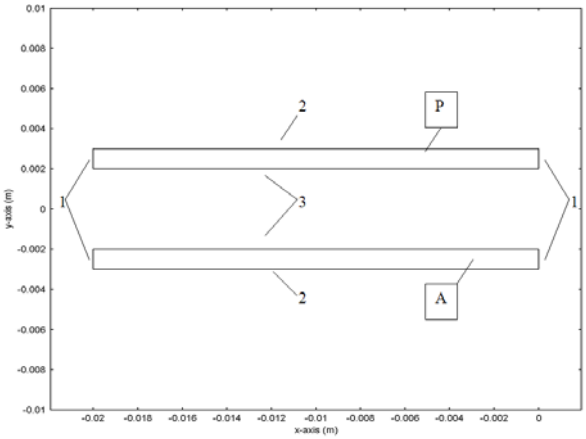

Fig. 1 Un-rotated model geometry and boundary conditions. Three types of boundary conditions were applied, boundaries were either: (1) constrained, (2) loaded, or (3) had contact conditions applied. Note, the lower structure (labelled *A*; *i.e.* anterior) was stiffer than the upper structure (labelled *P*; *i.e.* posterior)

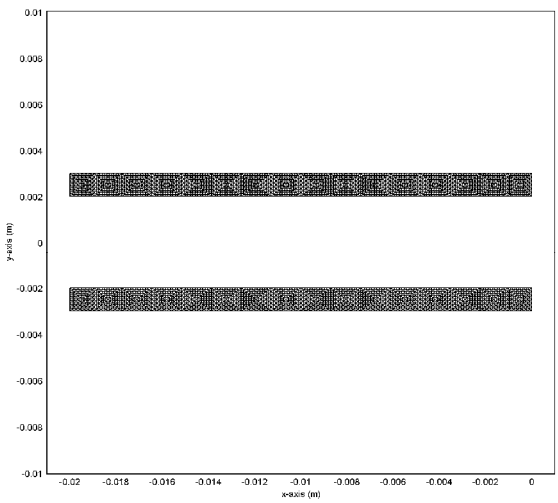

(a)

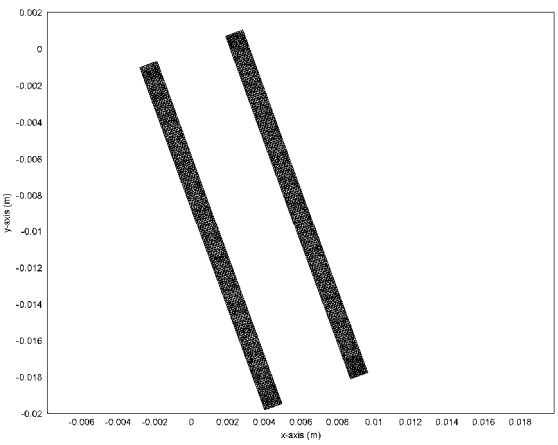

(b)

Fig. 2 Applied mesh. Mesh applied to model when (a) not rotated and (b) when rotated at a clockwise rotation angle, with respect to the *x-axis*, of 255°

2.2 Contact Modelling

2.2.1 Contact Using Symmetry Across an Axis of a Cartesian Coordinate System

The magnitude of the contact force at a boundary, *B*, was previously determined [1-3] using Eq. 1.

$$\begin{aligned} B &= \tau - gC\ , \quad g < 0 \\ B &= \tau e^{-g(C/\tau)}\ , \quad g \geq 0 \end{aligned} \tag{1}$$

Here τ is an approximation of the contact force, *C* is a large constant (1×10^9), *B* is the contact force at each node. The value of *g* is calculated using Eq. 2.

$$g = x_A + x_P \tag{2}$$

Here the two variables x_A and x_P define the displacement of any node along the contact boundary as defined by Eqs. 3 and 4, respectively. Subscripts *A* and *P* refer to contact boundaries of the two separate, contacting, structures. Then

$$x_A = -x_{Ao} - \delta x_A \tag{3}$$

$$x_P = x_{Po} + \delta x_P \tag{4}$$

where x_{Ao} and x_{Po} define the initial *x-axis* coordinate, and δx_A and δx_P define the displacement along this axis for contacting structures/boundaries *A* and *P*, respectively.

2.2.2 Arbitrary Position for Contact

For contact in an arbitrary position, the gap expression (Eq. 2) is modified to Eq. 5, so that the gap normal to the contact boundaries is calculated.

$$g = g_o - (n_A + n_P) \tag{5}$$

Here g_o defines the gap normal to the two contacting boundaries (Eq. 6), n_A and n_P define the normal displacement of nodes along the contacting boundaries *A* (Eq. 7) and *P* (Eq. 8), respectively. Then

$$g_o = \left[(y_{Ao} - y_{Po})^2 + (x_{Ao} - x_{Po})^2 \right]^{1/2} \tag{6}$$

where x_{Ao}, x_{Po}, y_{Ao} and y_{Po} refer to the original *x*- and *y*-axis coordinates for nodes along contact boundaries *A* and *P*, respectively.

$$n_A = u_A + v_A \tag{7}$$

$$n_P = u_P + v_P \tag{8}$$

In Eqs. 7 and 8, u_A, v_A, u_P and v_P refer to the component of displacement in the *x*-and *y*-axis directions of the contact boundaries for nodes along contact boundaries *A* and *P*, respectively, normal to the contact boundary.

The contact method requires the definition of 'boundary extrusion variables' in Comsol multi-physics. Each boundary requires node position and displacement (n_A, n_P and *x*- and *y*- coordinates) to be made available. In the model defined in sections 2.3 to 2.7 sliding was assumed negligible (by linearly extruding variables

from one contact boundary to the other). However, the contact method presented (above) is also applicable to models where sliding is not neglected, as defined previously [1]. Note, in that case previous definitions for *y*-axis translation should be replaced by displacement tangential to the contacting boundaries.

2.3 Geometry

The model solved under contact conditions consists of two rectangles of equal length (20mm) and width (1mm). The two structures were placed 4mm apart (Fig. 1). This geometry mimicked conditions for contact of certain heart valves [1]; further details for the valves chosen are provided elsewhere [4]. The model was rotated clockwise from the origin of the coordinate system with respect to the *x*-axis (parallel to the contacting boundaries in the un-rotated model), by 15°, 30°, 45°, 60°, 75°, 90° and 255° (Fig. 2).

2.4 Boundary Conditions

Contacting structures were restrained at their shorter boundaries, contacting boundaries had contact conditions applied (section 2.2), and a force was applied to the remaining boundary of each structure (Fig. 1). A force per unit area of 20kN/m^2 was applied normal to the boundary (assuming a thickness of 0.01m).

2.5 Material Properties

The two contacting structures were simulated as linearly elastic and isotropic, with properties determined for heart valve leaflets [5] using a protocol for testing similar components [6]. The two contacting structures had different material properties. One structure (*A* in Fig. 1) had a Young's modulus of 2MPa, but the other structure (*P* in Fig. 1) had a lower Young's modulus of 1MPa. Both structures had a Poisson's ratio of 0.33 and density of 1060kg/m^{-3}.

2.6 Meshing

The default 'normal' mesh was applied using a free meshing approach (Table 1, Fig. 2). The automated meshing approach led to minor differences in the number of model elements.

2.7 Analysis

FEA was performed using the structural mechanics package of Comsol multi-physics (v3.3, Comsol Ltd, Cambridge, UK). This package enables large deformations to be calculated and determines Green strains and Cauchy stresses. A direct UMFPACK solver was used for all solutions. Further solver settings were consistent with those applied in a previous study [1].

3. RESULTS

The stiffer structure deformed the least of the two contacting structures (Fig. 3). Stresses in the deformed structures concentrated at their restrained edges

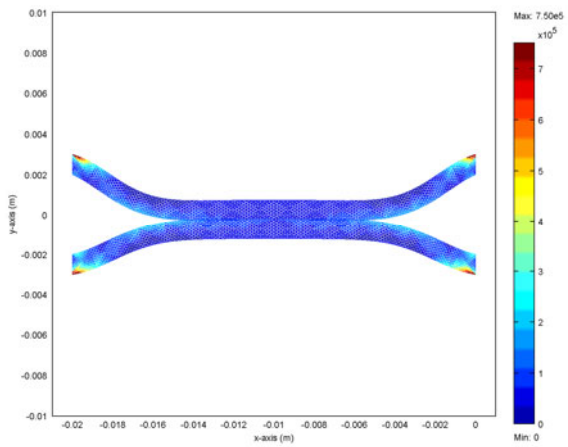

Fig. 3 Deformation and von Mises stress (Pa) distribution at a clockwise rotation angle, with respect to the *x-axis*, of 0° (*i.e.* not rotated). The scale bar denotes von Mises stress (Pa)

Table 1 Element type, number and total degrees of freedom solved for at a range of clockwise rotation angles, with respect to the *x-axis*

Model rotation angle (°)	Total degrees of freedom solved	Number of Elements	Lagrange element type
0	676	128	Quadratic
15	636	120	Quadratic
30	676	128	Quadratic
45	716	136	Quadratic
60	676	128	Quadratic
75	636	120	Quadratic
90	676	128	Quadratic
255	636	120	Quadratic

(Fig. 3). Peak von Mises stress was 946kPa when the structures were oriented at 0°. This peak stress ranged from 941kPa to 947kPa with model orientation, with the higher value at 60° orientation (Table 2). The minimum value varied between 6.8kPa to 7.9kPa (Table 2).

Cauchy stresses and Green strains are oriented along the *x*- and *y*-axes of the coordinate system. Therefore, these varied with the model orientation. However, equivalent values on opposing axes were predicted by models which were mirrored along an axis (Table 2). For example, at an orientation of 15° peak Cauchy stresses were 1019kPa and 423kPa along the *x*- and *y*-axis, respectively, compared to 423kPa and 1019kPa respectively when the model had an orientation of 75°.

Contact occurred over most of the contacting boundaries, except towards the edges. Peak contact pressure occurred towards the central portion of the contact boundaries (Fig. 4). Peak contact pressure was 23kPa. This value varied with orientation from 22.66kPa and 22.77kPa depending on the model orientation (Table 2).

Contact pressure was symmetrically distributed along the contacting boundaries (Fig. 5). Peak contact pressure occurred at 7mm and 13mm along the boundary length. At 3mm and 17mm along the boundary length the contact pressure fell to virtually zero (Table 2). This was independent of the orientation of the leaflets with respect to the *x*- and *y*- axes.

4. DISCUSSION

This paper provides a method to define contact between boundaries where the structures are not aligned to the predefined axes in Comsol Multi-physics. The need for improved contact modelling with this software has been previously defined, in terms of limited transient contact modelling [1,7]. Due to such limitations, a method to enable transient large strain contact modelling was developed [1]. However, this method required symmetry about an axis. In this paper, we provide a method to enable such contact without assuming symmetry.

The results presented demonstrate that overall model predictions did not change with model orientation. The differences between models, *e.g.* 0.11kPa for contact pressure and 6kPa for von Mises stress, are likely due to the minor differences in the number of elements

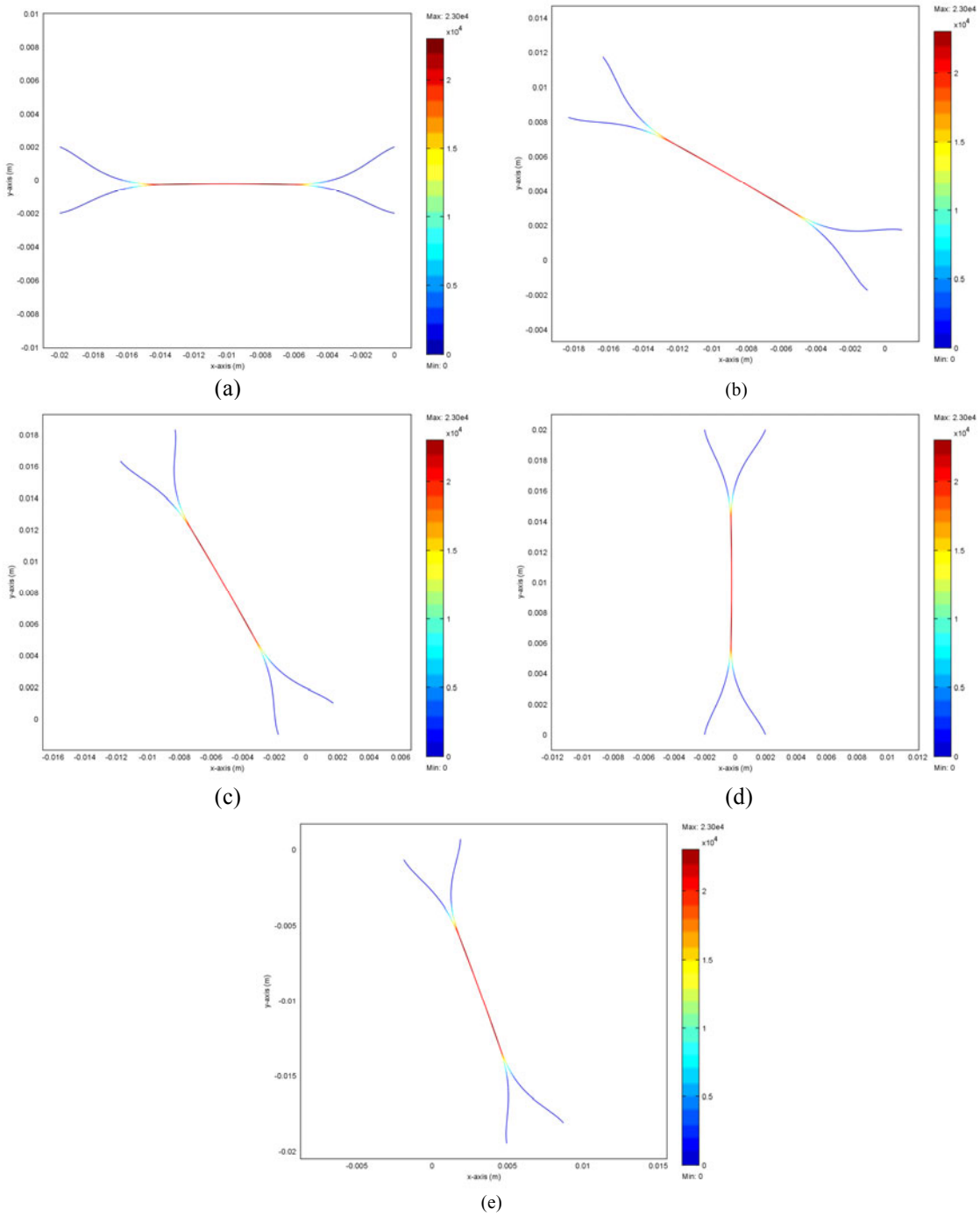

Fig. 4 Contact pressure distribution along the two contacting boundaries at clockwise rotation angles, with respect to the *x-axis*, of (a) 0°, (b) 30°, (c) 60°, (d) 90°, (e) 255°. The scale bar denotes contact pressure (Pa)

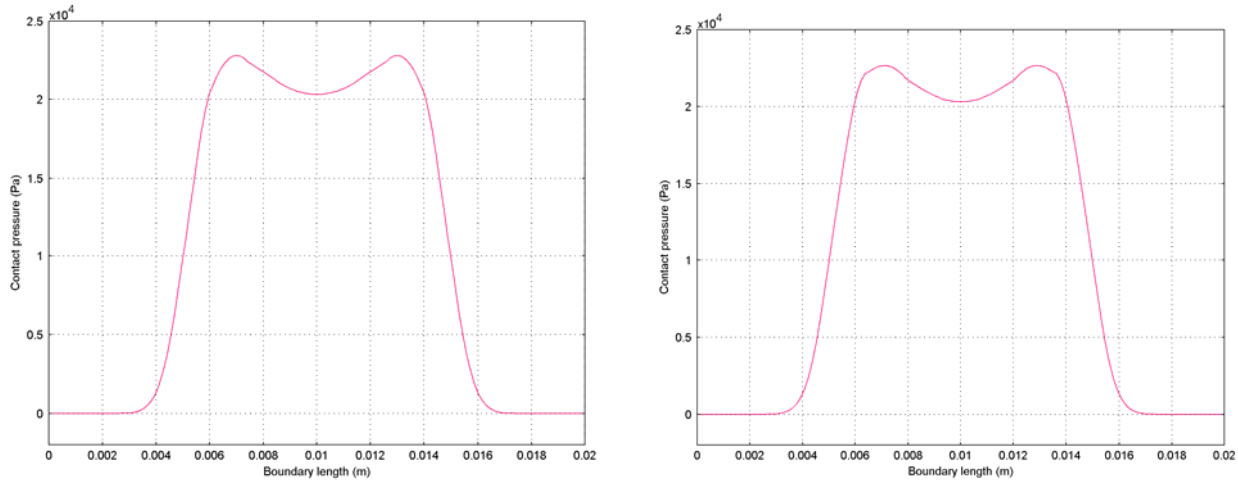

(a) (b)

Fig. 5 Contact pressure distribution along contacting boundary of the stiffer structure at clockwise rotation angles, with respect to the *x-axis*, of (a) 0°, (b) 255°

Table 2 Stress, strain and contact pressures determined for the model at a range of clockwise rotation angles, with respect to the *x-axis*

Model rotation angle (°)		von Mises (kPa)	Cauchy stress (kPa)				Green strain			Contact pressure (Pa)
			σ_x	σ_y	σ_z	σ_{xy}	ε_x	ε_y	ε_{xy}	
0	max	945.6	939.5	252.1	227.0	383.7	0.46	0.17	0.12	22.8×10^3
	min	7.9	−347.4	−234.6	−236.9	−383.7	−0.32	−0.19	−0.12	4.1×10^{-5}
15	max	941.4	1018.6	422.9	226.2	160.8	0.47	0.17	0.17	22.7×10^3
	min	6.8	−346.9	−249.1	−236.4	−496.5	−0.31	−0.21	−0.26	4.1×10^{-5}
30	max	946.7	1029.7	696.1	227.6	158.8	0.40	0.17	0.24	22.8×10^3
	min	7.9	−331.6	−275.2	−237.0	−494.5	−0.25	−0.13	−0.34	4.1×10^{-5}
45	max	946.0	913.7	913.7	227.7	175.1	0.26	0.26	0.24	22.7×10^3
	min	7.0	−305.1	−305.1	−236.9	−409.0	−0.15	−0.15	−0.33	4.1×10^{-5}
60	max	946.7	696.1	1029.7	227.6	158.8	0.17	0.40	0.24	22.8×10^3
	min	7.9	−275.2	−331.6	−237.0	−494.5	−0.13	−0.25	−0.34	4.1×10^{-5}
75	max	941.4	422.9	1018.6	226.2	160.8	0.17	0.47	0.17	22.7×10^3
	min	6.8	−249.1	−346.9	−236.4	−496.5	−0.21	−0.31	−0.26	4.1×10^{-5}
90	max	945.6	252.1	939.5	227.0	383.7	0.17	0.46	0.12	22.8×10^3
	min	7.9	−234.6	−347.4	−236.9	−383.7	−0.19	−0.32	−0.12	4.1×10^{-5}
255	max	941.3	510.5	1024.9	226.2	127.1	0.15	0.46	0.20	22.7×10^3
	min	6.8	−256.9	−343.5	−236.3	−506.5	−0.19	−0.29	−0.30	4.1×10^{-5}

between models. This is due to the use of an automated mesh. However, these differences were minimal given the predicted values (*i.e.* differences of 0.4% and 0.6% for peak contact pressure and stress, respectively). This demonstrates that the contact method is consistent regardless of orientation. However, any model that applied contact modelling would require subsequent validation.

When compared to our study with a comparable model [1], minor differences were predicted. In this current study peak von Mises stresses were in the range of 0.95MPa, in the previous study such stresses were 1.2MPa. Peak contact pressure in this study was 23kPa, compared to around 30kPa in the previous study. These differences are likely caused by neglecting sliding in this current model. When sliding is not accounted for, deflection parallel to the contact boundary leads to an underestimation of the gap between contact boundaries, thereby underestimating the contact pressure. In our current model, stresses and contact pressure were lower than in the previous model where sliding was accounted for; *i.e.* consistent with sliding being ignored in the current method. This simplification has been used to provide clarity when describing the contact method between structures with an arbitrary location with respect to a coordinate system. The intention is to aid readers aiming to implement this contact method. However, the method presented is compatible with the transient contact analysis that accounts for sliding, as defined previously [1].

The contact method was originally developed to enable our time-dependent heart valve multi-physics

model [8] to include contact modelling [3]. However, the method is not limited to heart valve modelling and, in principle, the method is applicable to objects with more complicated geometries than for the example in this paper. For example, this method can be applied to modelling joints in the body which have complicated three-dimensional shapes [9]. This is because these joints are covered by articular cartilage which, despite large deformation when in contact with an opposing surface, allows smooth motion and has a surface roughness of 165 to 174nm [10]. More widely, though, difficulties for contact modelling of elasto-plastic materials have been reported [7]. The contact method described is of most use for contact modelling where time dependency is important. Therefore, modelling of viscoelastic materials and their properties and their time-dependency during contact is another potential application of this contact method. The contact method presented has been developed using Comsol multi-physics due to its capabilities for multi-physics modelling, and this method is compatible within any combination of multi-physics problems allowed using that software. However, as the contact is described using equations, this contact method can be used in most finite element packages.

ACKNOWLEDGMENTS

The authors would like to thank the British Heart Foundation for a Junior Fellowship (FS/05/32) awarded to DME during the early stages of this investigation. The research leading to these results has received funding from the [European Community's] Seventh Framework Programme [FP7/2007-2013] under a Marie Curie Intra-European Fellowship for Career Development, grant agreement n° [252278], awarded to DME.

REFERENCES

1. Espino, D. M., Shepherd, D. E. T. and Hukins, D. W. L, "Development of a Transient Large Strain Contact Method for Biological Heart Valve Simulations," *Computer Methods in Biomechanics and Biomedical Engineering*, In Press DOI: 10.1080/10255842.2011.623676 (2012).
2. Espino, D. M., Shepherd, D. E. T. and Hukins, D. W. L., "Transient Large Strain Contact Modelling: A Comparison of Contact Technique for Simultaneous Fluid-Structure Interaction," *Computers and Fluids*, Submitted (2011).
3. Espino, D. M., Shepherd, D. E. T. and Hukins, D. W. L., "Evaluation of a Transient, Simultaneous, Arbitrary Lagrange Euler Based Multi-Physics Method for Simulating the Mitral Heart Valve," *Computer Methods in Biomechanics and Biomedical Engineering*, In Press DOI: 10.1080/10255842.2012.688818 (2012).
4. Al-Atabi, M., Espino, D. M., Hukins, D. W. L. and Buchan, K.G., "Biomechanical Assessment of Surgical Repair of the Mitral Valve," *Proceedings of the Institution of Mechanical Engineers*, Part H: Journal of Engineering in Medicine, **226**, pp. 275–287 (2012).
5. Kaur, H., "Determination of Material Properties of Natural Heart Valves," MEng Thesis, School of Mechanical Engineering, University of Birmingham, Birmingham, UK (2007).
6. Millard, L., Espino, D. M., Shepherd, D. E. T., Hukins, D. W. L. and Buchan, K. G., "Mechanical Properties of Chordae Tendineae: Variation with Chordal Type and Age," *Journal of Mechanics in Medicine and Biology*, **11**, pp. 221–230 (2011).
7. Pennec, F., Achkar, H., Peyrou, D., Plana, R., Pons, P. and Courtade, F., "Verification of Contact Modeling with Comsol Multiphysics Software," EUROSIM: Federation of European Simulation Societies, Slovenia (2007).
8. Al-Atabi, M., Espino, D. M. and Hukins, D. W. L., "Computer and Experimental Modelling of Blood Flow Through the Mitral Valve of the Heart," *Journal of Biomechanical Science and Engineering*, **5**, pp. 78–84 (2010).
9. Öhman, C., Espino, D. M., Heinmann, T., Baleani, M., Delingette, H. and Viceconti, M., "Subject-Specific Knee Joint Model: Design of an Experiment to Validate a Multi-Body Finite Element Model," *Visual Computer*, **27**, pp. 153–159 (2011).
10. Ghosh, S., Bowen, J., Jiang, K., Espino, D. M. and Shepherd, D. E. T., *Investigation of Techniques for the Measurement of Articular Cartilage Surface Roughness*, Micron, In Press. DOI: http://dx.doi.org/10.1016/j.micron.2012.06.007 (2012).

(Manuscript received August 7, 2012,
accepted for publication August 27, 2012.)